Biology of Reproduction, 2018, 98(4), 570–578
doi:10.1093/biolre/iox169
Research Article
Advance Access Publication Date: 11 December 2017

Research Article

Seipin deficiency leads to increased endoplasmic reticulum stress and apoptosis in mammary gland alveolar epithelial cells during lactation†

Ahmed E. El Zowalaty[1,2], Rong Li[1,2], Weiqin Chen[3] and Xiaoqin Ye[1,2,*]

[1]Department of Physiology and Pharmacology, College of Veterinary Medicine, University of Georgia, Athens, Georgia, USA; [2]Interdisciplinary Toxicology Program, University of Georgia, Athens, Georgia, USA and [3]Department of Physiology, Augusta University, Augusta, Georgia, USA

*__Correspondence__: Department of Physiology and Pharmacology, College of Veterinary Medicine and Interdisciplinary Toxicology Program, University of Georgia, Athens, GA 30602, USA. Tel: +1-706-542-6745; Fax: +1-706-542-3015; E-mail: ye@uga.edu

†__Grant Support:__ This study was funded by the National Institutes of Health (NIH R15HD066301 and NIH R01HD065939) (cofunded by ORWH and NICHD)) to XY.

Received 25 November 2017; Accepted 10 December 2017

Abstract

Seipin is an integral endoplasmic reticulum (ER) membrane protein encoded by Berardinelli–Seip congenital lipodystrophy type 2 (*BSCL2*/*Bscl2*) gene. Most litters (59%) from *Bscl2*$^{-/-}$ dams mated with wild type (WT) (*Bscl2*$^{+/+}$) males did not survive postnatal day 5 (PND5) and pups (*Bscl2*$^{+/-}$) lacked milk in their stomachs. The survived litters had reduced pup survival rate at PND21. It was hypothesized that seipin was critical for lactation. *Bscl2* was upregulated and highly detected in the lactation day 1 (LD1) WT mammary gland alveolar epithelial cells. LD1 *Bscl2*$^{-/-}$ mammary glands lacked adipocytes and alveolar clusters and had varied alveolar morphology: from interconnected mammary gland alveoli with dilated lumen and sloughed epithelial cells to undifferentiated mammary gland alveoli with unexpanded lumen. Comparable levels of whey acidic protein (WAP, a major component in rodent milk) staining and Nile Red lipid droplet staining between WT and *Bscl2*$^{-/-}$ LD1 alveolar epithelial cells indicated normal milk protein synthesis and lipid syntheses in LD1 *Bscl2*$^{-/-}$ mammary glands. Significantly reduced percentage of larger lipid droplets was detected in LD1 *Bscl2*$^{-/-}$ alveoli with unexpanded lumen. There was no obviously impaired proliferation detected by PCNA staining but increased apoptosis detected by cleaved caspase-3 staining in LD1 *Bscl2*$^{-/-}$ alveolar epithelial cells. Increased expression of protein disulfide isomerase and binding immunoglobulin protein in the LD1 *Bscl2*$^{-/-}$ mammary gland alveolar epithelial cells indicated increased ER stress. This study demonstrates increased ER stress and apoptosis in LD1 *Bscl2*$^{-/-}$ mammary gland alveolar epithelial cells and reveals a novel in vivo function of seipin in lactation.

Summary Sentence

Our findings that pups from *Bscl2*$^{-/-}$ dams lacked milk and had reduced survival rate as well as that LD1 *Bscl2*$^{-/-}$ mammary gland alveolar epithelial cells had increased ER stress and apoptosis reveal a novel in vivo function of seipin in lactation.

Key words: seipin, mammary gland alveolar epithelial cells, lactation, ER stress, apoptosis.

Introduction

The mammary gland undergoes tremendous side branching and alveologenesis to prepare for lactation [1]. A lactating mouse can secrete ~30 g of lipids in milk during the 20 days of lactation [2], and 98% of milk lipids are triglycerides [3]. A lactating mouse mammary gland can rapidly take up injected radiolabeled fatty acids and convert them into lipid droplets [4]. Microlipid droplets formed in the endoplasmic reticulum (ER) of a lactating mouse mammary gland consist of a triacylglycerol-rich core coated with a layer of proteins and polar lipids. This coating enhances aggregation of lipids into droplets. The lipid droplets are released from the ER in the mammary gland epithelium and fused with cytoplasmic lipid droplets, which are precursors of milk lipids [3] and are surrounded by the bilayer milk lipid globule membrane [5]. Endoplasmic reticulum is also the site for synthesis of milk proteins [6]. Interestingly, seipin is identified as a protein in the milk lipid globule membrane [7].

Seipin is an integral ER membrane protein encoded by Berardinelli–Seip congenital lipodystrophy type 2 (*BSCL2*/*Bscl2*) gene [8]. It has been shown that seipin physically interacts with the sarco/ER Ca^{2+}-ATPase in adipocytes [9]. Seipin is required for adipocyte differentiation and lipid droplet accumulation [8, 10–13]. Seipin deficiency results in lipodystrophy and muscle hypertrophy in human and mouse [10, 14–16]. Knockout of seipin in mice or in the fibroblasts of a human patient with seipin-based lipodystrophy results in small lipid droplets and an increase in the number of lipid droplets [17]. A recent study demonstrates that seipin is required for converting nascent to mature lipid droplets, possibly through seipin at ER-lipid droplet contact sites [18]. Milk production from lactation also involves lipid droplet formation [5]. Since seipin is involved in converting nascent to mature lipid droplets [18] and is a protein in the milk lipid globule membrane [7], it suggests that seipin might play a role in lactation.

We have been investigating the roles of seipin in pubertal development and reproduction using *Bscl2*$^{-/-}$ mice [15, 16]. Previously, we reported abnormalities in 5 weeks old *Bscl2*$^{-/-}$ mouse mammary glands, such as enlarged lymph nodes, longer and wider mammary gland ducts, and more terminal end buds [16], suggesting altered pubertal mammary gland development in *Bscl2*$^{-/-}$ mice and an in vivo role of seipin in mammary gland development. We also observed that many neonatal pups (*Bscl2*$^{+/-}$) from *Bscl2*$^{-/-}$ females mated with *Bscl2*$^{+/+}$ males died within a few days of birth. This observation promoted us to investigate *Bscl2*$^{-/-}$ mammary glands in lactation. Here, we reported a novel role of seipin in lactation.

Materials and methods

Animals

Bscl2$^{-/-}$ mice in C57BL/6J background were derived from an original colony at Baylor College of Medicine with backcrosses to C57BL/6J background for five generations [10]. Genotyping was done as previously described [15, 16]. *Bscl2*$^{+/+}$ (wild type, WT) and *Bscl2*$^{+/-}$ females were used as the genotype control for *Bscl2*$^{-/-}$ females. They were housed in polypropylene cages with free access to food and water on a 12 h light/dark cycle (0600–1800) at 23 ± 1°C with 30%–50% relative humidity at the College of Veterinary Medicine animal facility at the University of Georgia. The animals were sacrificed by CO_2 inhalation followed with cervical dislocation. At least three mice in each group were analyzed for each parameter. All methods used in this study were approved by the University of Georgia Institutional Animal Care and Use Committee (IACUC) Committee and conform to National Institutes of Health guidelines and federal law.

Litter size and survival

Young virgin control (*Bscl2*$^{+/+}$ and *Bscl2*$^{+/-}$) and *Bscl2*$^{-/-}$ females were mated with WT stud males. Pregnancy was determined by the increase of body weight (>30%) and the continuous changes of the belly shapes. Delivery was monitored and litter size at birth (postnatal day 1 [PND1]) from each dam was recorded. The litters were observed and the number of pups in each litter was recorded at weaning (PND 21). There were 53 litters from control dams and 22 litters from *Bscl2*$^{-/-}$ dams.

Lipid droplet analysis

Frozen sections (10 μm) of fourth inguinal mammary glands were stained with Nile Red (N3013, Sigma) in the dark for 20 min at room temperature and counterstained with 4′,6-Diamidino-2-Phenylindole, Dihydrochloride (DAPI). The sizes of all visible lipid droplets in representative areas (images with 80× magnification) on lactation day 1 (LD1, the day new pups were found) *Bscl2*$^{+/+}$ mammary glands and *Bscl2*$^{-/-}$ mammary glands (areas with expanded alveolar lumen and areas with less expanded/unexpanded alveolar lumen, indicated by denser nuclei in the DAPI staining) were quantified using ImageJ. The percentages of lipid droplets with readings >2000 and >1000 from each image were calculated for comparisons (N = 3–4 mice/group).

Histology and whole mount of mammary gland

The LD1 females were euthanized, and the mammary glands were dissected. The left side mammary glands were snap-frozen. The right fourth inguinal mammary gland was fixed in formalin, dehydrated in a series of 50%, 70%, 80%, 90%, 100% ethanol, and two changes of xylene, embedded in paraffin for histology. The right fourth inguinal mammary glands from another set of LD1 mice were used for whole mount as previously described [16, 19, 20]. The lumen area and epithelial area of all alveoli in a representative 40× image in each WT mammary gland, as well as a representative 40× image with expanded lumen and a representative 40× with less expanded/unexpanded lumen in each *Bscl2*$^{-/-}$ mammary gland were quantified using ImageJ. The ratio of lumen area to epithelial area of each alveolar was obtained. The average ratio of all alveoli in one 40× image represented one data point of each mouse (N = 3).

Table 1. A list of antibodies used in the study.

Antibody name	Catalog No.	Dilution	Company name
Protein disulfide isomerase (PDI)	Ab2792	1:200	Abcam
Cleaved caspase-3	Asp175	1:300	Cell Signaling
Proliferating cell nuclear antigen (PCNA)	D3H8P	1:1000	Cell Signaling
E-Cadherin (E-Cad)	24E10	1:300	Cell Signaling
Whey acidic protein (WAP)	SC-14832	1:200	Santa Cruz Biotechnology
Perilipin1 (Plin1)	(D1D8) XP Rabbit mAb #9349	1:200	Cell Signaling
Binding immunoglobulin protein (BiP)	Ab21685	1:200	Abcam

In situ hybridization

Sense and antisense cRNA probes were synthesized as previously described [15, 21]. The template for mouse *Bscl2* cRNA probe synthesis was amplified from m*Bscl2* cDNA using primers m*Bscl2*e3F: 5′-GTGCACTTCCACTACAGGAC-3′ and m*Bscl2*e6R: 5′-CTCCAGTTGTTGGCACATAC-3′. In situ hybridization was carried out as previously described [15, 21] on sections from gestation day 13.5 (D13.5, WT) and LD1 (WT and *Bscl2*$^{-/-}$) fourth inguinal mammary glands to demonstrate the regulation of *Bscl2*$^{+/+}$ from pregnancy to lactation and deletion of *Bscl2* in *Bscl2*$^{-/-}$ mammary gland.

Immunohistochemistry and immunofluorescence

Frozen sections (10 μm) of fourth inguinal mammary glands were used for immunohistochemistry and immunofluorescence as previously described [15, 22] using the following antibodies: anti-protein disulfide isomerase (PDI) antibody (1:200, ab2792, Abcam), anti-cleaved caspase-3 antibody (1:300, Asp175, Cell Signaling), anti-proliferating cell nuclear antigen (PCNA) antibody (1:1,000, D3H8P, Cell Signaling), anti-E-Cadherin (E-Cad) antibody (1:300, 24E10, Cell Signaling), anti-whey acidic protein (WAP) antibody (1:200, sc-14832, Santa Cruz Biotechnology), anti-perilipin1 (Plin1) antibody (1:200, (D1D8) XP Rabbit mAb #9349, Cell Signaling), and anti-GRP78/binding immunoglobulin protein (BiP) antibody (1:200, ab21685, Abcam) (Table 1).

Statistical analysis

Data are presented as mean ± SD wherever applicable. Two-tailed Fisher exact test was used for litter survival rate and pup survival rate. Two-tailed unequal variance Student *t*-test was used for litter size, percentage of larger lipid droplets, and cleaved caspase-3 quantification. Ranking test coupled with two-tailed unequal variance Student *t*-test was used for ratios of alveolar lumen area/epithelial area. Significance level is set at $P < 0.05$.

Results

Bscl2$^{-/-}$ females have impaired lactation

Bscl2$^{-/-}$ females had comparable mating activity with age-matched control females when they were mated with WT (*Bscl2*$^{+/+}$) stud males. The average numbers and sizes of implantation sites examined on gestation day 13.5 were comparable between control and *Bscl2*$^{-/-}$ females [23], indicating no obvious defects in early pregnancy events, such as ovulation, fertilization, embryo development, embryo implantation, and placental development in *Bscl2*$^{-/-}$ dams. However, among the 22 litters delivered by *Bscl2*$^{-/-}$ females (2–4 months old, mated with WT stud males), 13 of them had 1–10 pups per litter at birth (PND1) but all live pups at birth in these

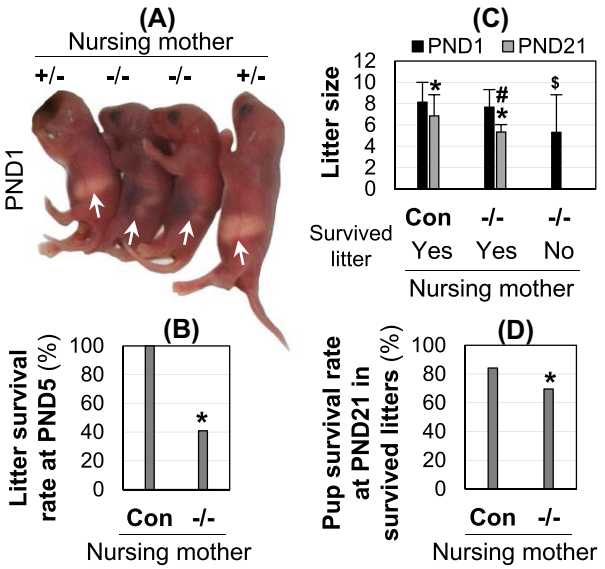

Figure 1. Litter sizes and litter survival rates. (A) PND1 pups from *Bscl2*$^{+/-}$ (+/–) and *Bscl2*$^{-/-}$ (–/–) dams. White arrows indicated milk spots in the stomachs. (B) Litter survival rates from control (Con: +/+ and+/–, N = 53) and *Bscl2*$^{-/-}$ (–/–, N = 22) nursing mothers (*$P < 0.05$). (C) Litter sizes at PND1 and PND21. N = 53 survived litters from control nursing mothers, nine survived litters from –/– nursing mothers, and 13 deceased litters from –/– nursing mothers. *$P < 0.05$, compared to respective PND1; #$P < 0.05$, compared to PND21 control; $$P < 0.05$, compared to the other two PND1 litter sizes; error bar, standard deviation. (D) Pup survival rate at PND21 in the survived litters. N = 431 pups in 53 survived litters from control nursing mothers, and 69 pups in nine survived litters from –/– nursing mothers; *$P < 0.05$.

13 litters were dead by PND5 due to lack of milk in their stomachs (Figure 1A). The remaining 9 litters from *Bscl2*$^{-/-}$ females survived PND5 and were weaned at PND21. Therefore, the litter survival rate from *Bscl2*$^{-/-}$ dams (9/22 = 40.9%, $P < 0.0001$) was significantly decreased compared to the control (*Bscl2*$^{+/+}$ and *Bscl2*$^{+/-}$, 53/53 = 100%) (Figure 1B). The nine survived litters from *Bscl2*$^{-/-}$ dams had comparable litter size at PND1 to that from the control dams but had significantly decreased litter size at PND21 compared to that from the control dams (Figure 1C), indicating reduced pup (*Bscl2*$^{+/-}$) survival rate in the survived litters from *Bscl2*$^{-/-}$ dams (Figure 1D). The litter sizes at PND21 in both groups were significantly lower than their respective litter sizes at PND1 (Figure 1C). When newborn pups (*Bscl2*$^{+/-}$, N = 5) from *Bscl2*$^{-/-}$ dams (mated with WT stud males) were fostered by postpartum day 1 WT females, all of them survived. The reduced pup (*Bscl2*$^{+/-}$) survival rate in the survived litters from *Bscl2*$^{-/-}$ dams (Figure 1D) and the observation that some milk was seen in the stomachs of the live pups

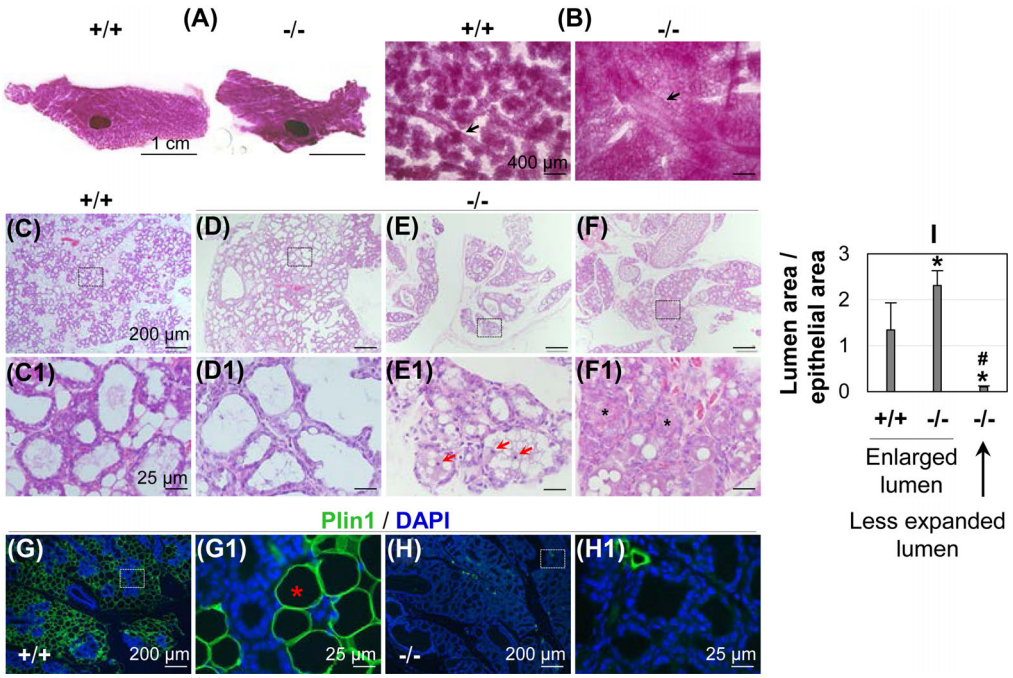

Figure 2. Whole mount, histology, and perilipin1 (Plin1) immunofluorescence of LD1 WT (+/+) and *Bscl2*$^{-/-}$ (–/–) mammary glands. (A and B) Whole mount. Black arrows in B, mammary gland ducts. (C–F1) Histology; (C1–F1) enlarged from the rectangle areas in C–F, respectively. Red arrows in E1, sloughed alveolar epithelial cells; black stars in F1, unexpanded alveolar lumen. (G–H1) Plin1 immunofluorescence. (G1–H1) Enlarged from the rectangle areas in G and H, respectively. Green, Plin1 staining of adipocytes (red star); blue, counterstaining with DAPI; scale bars, 1 cm (A), 400 μm (B), 200 μm (C–H), or 25 μm (C1–H1). (I) Ratios of lumen area/epithelial area. $^{*}P < 0.05$, compared to +/+; $^{\#}P < 0.05$, compared to –/– with enlarged lumen; N = 3; error bar, standard deviation.

from *Bscl2*$^{-/-}$ dams that were dead by PND5 (Figure 1A) suggested insufficient milk production from the *Bscl2*$^{-/-}$ mothers.

Bscl2$^{-/-}$ mammary gland histology

Whole mount LD1 mammary glands showed alveolar clusters in the WT females but not in the *Bscl2*$^{-/-}$ females, which had mammary gland alveoli spread out more like a sheet instead of clusters (Figure 2A and B). The LD1 *Bscl2*$^{-/-}$ mammary glands also had enlarged ducts (Figure 2B). Histology confirmed the clusters of secretory mammary gland alveoli that were surrounded by adipocytes, indicated by perilipin1 (Plin1), a lipid droplet associated protein [24], in the LD1 WT mammary glands (Figure 2C, C1, G and G1). The appearances of the alveoli in the LD1 *Bscl2*$^{-/-}$ mammary glands varied greatly: some had mammary gland alveoli interconnected with dilated lumen (Figure 2D and D1), some had small mammary gland lobules with heterogeneity in the expansion of alveolar lumen and sloughed epithelial cells in the lumen (Figure 2E and E1), while others had small mammary gland lobules and nonsecretory alveoli with unexpanded lumen (Figure 2F and F1). Those with dilated lumen had higher lumen area/epithelial area ratio compared to WT, while those with unexpanded lumen had significantly lower lumen area/epithelial area ratio (Figure 2I). There was interlobular connective tissue but generally absent of adipocytes in the LD1 *Bscl2*$^{-/-}$ mammary glands, despite the scattered Plin1 staining (Figure 2D–F, D1–F1, H and H1). The lack of adipocytes in the mammary gland was consistent with lipodystrophy in the *Bscl2*$^{-/-}$ females [16].

Expression of *Bscl2* in lactation day 1 mammary glands

In situ hybridization indicated that *Bscl2* had a relatively low level of expression in the D13.5 WT mammary gland (Figure 3A). *Bscl2* was upregulated and highly detected in the LD1 WT mammary gland alveolar epithelial cells (Figure 3B and D). It appeared that *Bscl2* was also detectable in the WT adipocytes, but at a much lower level than in the LD1 WT alveolar epithelial cells (Figure 3A and B). The same *Bscl2* antisense probe also detected some signals in the LD1 *Bscl2*$^{-/-}$ mammary gland (Figure 3C), but the signals were much weaker than that in the LD1 WT mammary gland (Figure 3B). No specific signal was detected in an LD1 WT mammary gland using a sense *Bscl2* probe (Figure 3E). The high expression of *Bscl2* in the LD1 WT mammary gland epithelial cells suggested a local function of *Bscl2* in the mammary gland epithelium.

Expression of whey acidic protein in lactation day 1 mammary gland

The observations of insufficient milk in pups' stomachs (Figure 1A) and reduced postnatal pup survival rate (Figure 1D) suggested insufficient milk production in the *Bscl2*$^{-/-}$ mammary glands. To determine milk protein production in the *Bscl2*$^{-/-}$ LD1 mammary gland alveolar epithelial cells, WAP, a major component in rodent milk [25], was examined in LD1 mammary gland frozen sections using immunofluorescence. WAP was detected in all mammary gland epithelial cells with more intense labeling on the apical side of epithelial cells in the LD1 WT mammary glands (Figure 4A–C and J). Similar WAP expression pattern was also detected in the LD1 *Bscl2*$^{-/-}$ mammary gland epithelial cells with enlarged alveolar lumen (Figure 4D and F). However, in the alveoli with unexpanded lumen, WAP was detected more on apical side of epithelial cells in some alveoli (Figure 4K) but such stronger apical WAP staining was not obvious in other alveoli without expanded lumen (Figure 4G–I and L). There appeared to have no obvious difference in the expression

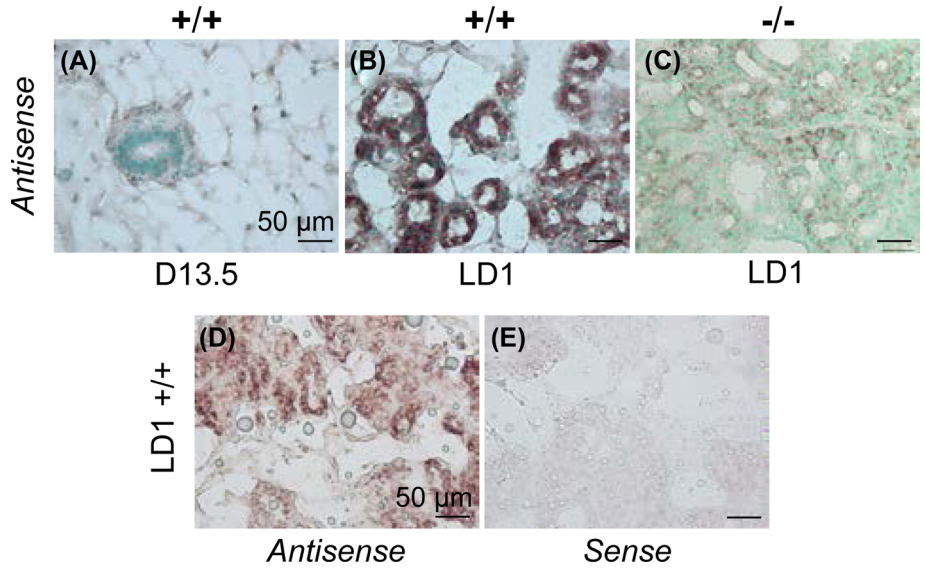

Figure 3. Detection of *Bscl2* mRNA in gestation day 13.5 (D13.5) WT (+/+) and LD1 mammary glands by in situ hybridization. (A) D13.5 WT, antisense probe. (B) LD1 WT, antisense probe. (C) LD1 *Bscl2*$^{-/-}$, antisense probe. (A–C) Sections were counterstained with methyl green. (D) LD1 WT, antisense probe. (E) LD1 WT, sense probe. Scale bar, 50 μm.

level of WAP in the mammary gland epithelial cells between WT and *Bscl2*$^{-/-}$ LD1 mammary glands (Figure 4). No specific signal was detected in the negative control (data not shown). These data demonstrated no defective synthesis of WAP in the *Bscl2*$^{-/-}$ LD1 mammary gland alveolar epithelial cells.

Lipid droplets in lactation day 1 *Bscl2*$^{-/-}$ mammary gland

In addition to milk protein, another important component of milk is fat. Nile Red lipid droplet staining of frozen LD1 mammary gland sections showed some very large fluorescent irregular smears in the WT that were absent from LD1 *Bscl2*$^{-/-}$ mammary gland sections (Figure 5). These smears most likely indicated adipocytes that were absent from the LD1 *Bscl2*$^{-/-}$ mammary gland (Figure 2). Although the LD1 mammary gland structures differed greatly (Figure 2), the density of lipid droplets appeared comparable between LD1 WT and *Bscl2*$^{-/-}$ mammary glands in areas with alveoli (Figure 5). The sizes of the lipid droplets varied greatly in both WT and *Bscl2*$^{-/-}$ LD1 mammary glands (Figure 5). Quantitative data (Figure 5J) revealed that the percentage of larger lipid droplets (with ImageJ reading > 1000) in the areas of *Bscl2*$^{-/-}$ LD1 mammary glands with expanded alveolar lumen (Figure 5D–F) was comparable with that of *Bscl2*$^{+/+}$ LD1 mammary glands (Figure 5A–C), while significantly higher than that in the areas of *Bscl2*$^{-/-}$ LD1 mammary glands with less expanded/unexpanded alveolar lumen, indicated by denser nuclei in the DAPI staining (Figure 5G–I). These data indicated that lipid synthesis was not impaired but lipid droplet aggregation might be impaired in the *Bscl2*$^{-/-}$ mammary gland with undifferentiated alveoli.

Alveolar epithelial cell proliferation and apoptosis in lactation day 1 *Bscl2*$^{-/-}$ mammary gland

Since milk protein WAP synthesis and lipid synthesis in the *Bscl2*$^{-/-}$ mammary glands were not obviously impaired, to find out the causes for reduced milk production, cell proliferations and apoptosis in the LD1 mammary glands were detected by PCNA staining and cleaved caspase-3 staining, respectively. Almost all alveolar epithelial cells (with round nuclei) were PCNA positive in both WT and *Bscl2*$^{-/-}$ LD1 mammary glands (Figure 6A, B1 and B2). However, some *Bscl2*$^{-/-}$ LD1 alveoli had less PCNA positive epithelial cells (Figure 6B2) because these alveoli lacked epithelial cells (Figure 6B2, D3 and H), most likely due to increased apoptosis (Figure 6D3). Cleaved caspase-3 positive cells were rarely detected in the WT LD1 mammary gland alveoli (Figure 6C) but more frequently detected in the *Bscl2*$^{-/-}$ LD1 mammary gland alveoli (Figure 6D), which could be in the epithelial cells on the alveolar epithelium (Figure 6D1), or detached epithelial cells in the alveolar lumen (Figure 6D2 and D3). All the cleaved caspase-3 positive cells were alveolar epithelial cells in both WT and *Bscl2*$^{-/-}$ LD1 mammary glands. Quantification of total cleaved caspase-3 positive cells per 10× image (Figure 6E) or per 10^4 nuclei (counted by ImageJ) (Figure 6F) showed over 10-fold increase of cleaved caspase-3 positive cells in the *Bscl2*$^{-/-}$ alveoli. Some LD1 *Bscl2*$^{-/-}$ alveoli had a few or were depleted of epithelial cells (Figure 6D3), which could explain reduced number of cells with round nuclei in the PCNA staining (Figure 6B2). E-Cad staining revealed organized alveolar epithelial cells in the LD1 WT mammary gland (Figure 6G), but disorganized and often "flattened" or absent, especially in the alveoli with dilated lumen and sloughed epithelial cells, in the LD1 *Bscl2*$^{-/-}$ mammary gland (Figure 6H). The *Bscl2*$^{-/-}$ alveoli with scattered epithelial cells or depletion of epithelial cells most likely resulted from epithelial cell apoptosis as seen in Figure 6D3. These data indicated normal alveolar epithelial cell proliferation but increased alveolar epithelial cell apoptosis in the *Bscl2*$^{-/-}$ LD1 mammary glands.

Endoplasmic reticulum stress in lactation day 1 *Bscl2*$^{-/-}$ mammary gland

Since seipin is localized in the ER and mutant forms of seipin can activate the unfolded protein response (UPR) pathway and induce ER stress-mediated cell death in cultured cells [26], it was hypothesized that seipin deficiency in the *Bscl2*$^{-/-}$ mammary gland caused ER stress leading to apoptosis in the alveolar epithelial cells. To test

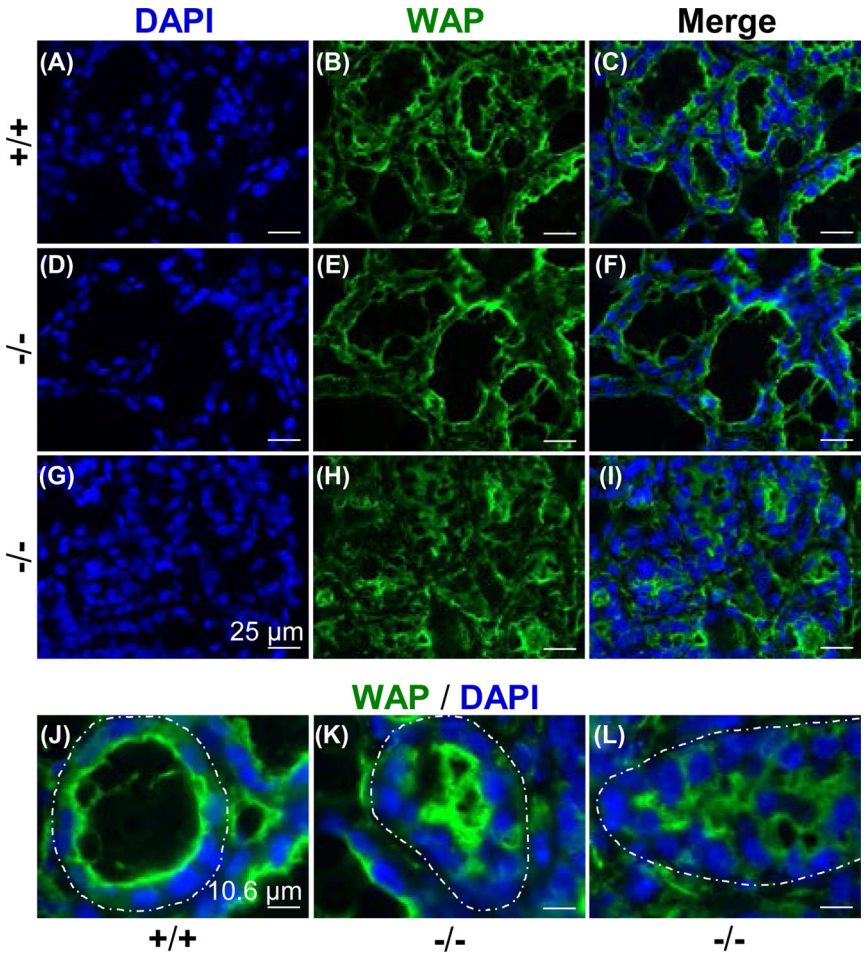

Figure 4. Detection of WAP in LD1 mammary glands. (A–C) Wild type (+/+). (D–F) *Bscl2*$^{-/-}$ (–/–) LD1 mammary gland with enlarged alveolar lumen. (G–I) *Bscl2*$^{-/-}$ (–/–) LD1 mammary gland with unexpanded alveolar lumen. Scale bar, 25 μm (A–I). (J–L) Zoom-in images of a WT (+/+) alveolus with expanded lumen showing apical WAP staining (J), two *Bscl2*$^{-/-}$ (–/–) alveoli without expanded lumen showing stronger apical WAP staining (K) and relatively even cytoplasm WAP staining (L), respectively. White broken line, outline of an alveolus; scale bar, 10.6 μm.

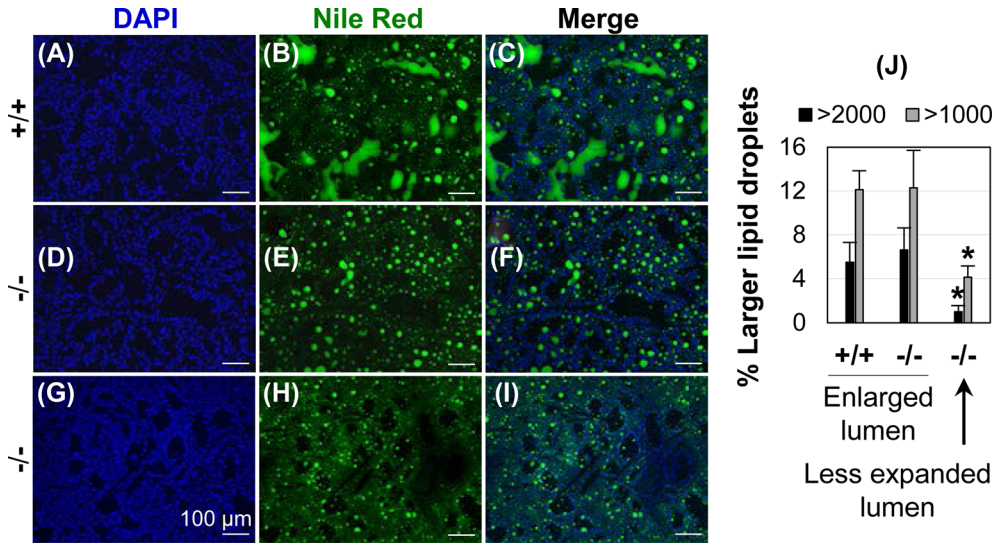

Figure 5. Detection of lipid droplets in LD1 mammary glands using Nile Red staining. (A–C) Wild type (+/+). (D–F) *Bscl2*$^{-/-}$ (–/–) LD1 mammary gland with enlarged alveolar lumen. (G–I) *Bscl2*$^{-/-}$ (–/–) LD1 mammary gland with less expanded/unexpanded alveolar lumen. Green dots, Nile Red staining of lipid droplets; blue: DAPI staining of nuclei; scale bar, 100 μm. (J) Percentage of larger lipid droplets with ImageJ readings >2000 or >1000. The three sets of data corresponded to the scenarios in B, E, and H, respectively. N = 3–4 mice/group; $^{*}P < 0.05$; error bar, standard deviation.

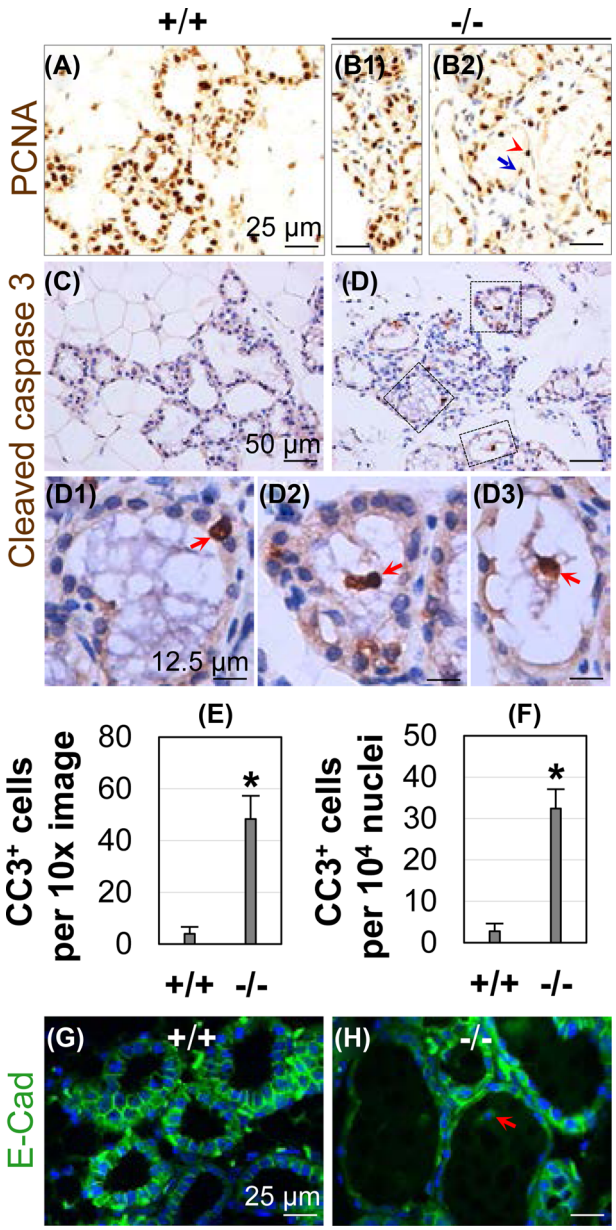

Figure 6. Detection of PCNA, cleaved caspase-3, and E-Cad in LD1 mammary glands using immunohistochemistry or immunofluorescence. (A–B2) PCNA. Red arrowhead in B2, an alveolar epithelial cell; blue arrowhead in B2, a myoepithelial cell. (C–D3) Cleaved caspase-3. (D1–D3) Enlarged from the rectangle areas in D; red arrows, cleaved caspase-3 positive cells in the alveolar epithelium and lumen. (E–F) Quantification of cleaved caspase-3 positive ($CC3^+$) cells per 10× image (E) or per 10^4 nuclei (F). N = 3 mice/group; $^*P < 0.05$; error bar, standard deviation. (G–H) Merged images of E-Cad (green) and DAPI (blue) staining. Red arrow in F, sloughed epithelial cell in alveolar lumen.

this hypothesis, PDI and BiP, two ER chaperones induced during ER stress and important players in UPR pathway [26, 27], were examined in the LD1 WT and *Bscl2*$^{-/-}$ mammary glands. PDI was detected in the cytoplasm of all alveolar epithelial cells. The expression of PDI in WT alveoli was relatively comparable among all epithelial cells except stronger signal in a few cells (Figure 7A–C). The PDI signal in many LD1 *Bscl2*$^{-/-}$ alveolar epithelial cells was much stronger than that in the WT epithelial cells regardless of their localizations in the alveoli with most retained epithelial cells (Figure 7D–F) or in the alveoli with a few remaining epithelial cells (Figure 7G–I). Detached *Bscl2*$^{-/-}$ alveolar epithelial cells in the lumen appeared to have weaker PDI staining than those attached epithelial cells (Figure 7G–I). Similar pattern of BiP upregulation in LD1 *Bscl2*$^{-/-}$ alveolar epithelial cells was also observed (Figure 7J–L). These results indicated increased ER stress in the LD1 *Bscl2*$^{-/-}$ alveolar epithelial cells.

Discussion

This study reveals a novel in vivo role of seipin in lactation. Two main categories of components in the milk are proteins and lipids, which are originally produced in the mammary alveolar epithelial cells. Most litters (59%) from *Bscl2*$^{-/-}$ dams failed to survive PND5, and the survived litters had reduced postnatal survival rate, indicating insufficient milk production from the *Bscl2*$^{-/-}$ mothers. However, the expression level of WAP (a major component in rodent milk [25]) and the density of lipid droplets in the LD1 *Bscl2*$^{-/-}$ mammary alveolar epithelial cells appeared comparable to control, indicating that the *Bscl2*$^{-/-}$ mammary alveolar epithelial cells were functional in protein synthesis and lipid synthesis for milk production. This study demonstrates abnormal morphology in LD1 *Bscl2*$^{-/-}$ mammary alveoli: from undifferentiated and nonsecretory alveoli with unexpanded lumen to alveoli with dilated lumen and sloughed epithelial cells. These conditions compromise milk production in the *Bscl2*$^{-/-}$ mammary gland.

Seipin is an integral ER membrane protein [8] that is required for adipocyte differentiation and lipid droplet accumulation [8, 10–13]. However, heterogeneities in cell differentiation and lipid droplet accumulation were observed in the LD1 *Bscl2*$^{-/-}$ mammary gland epithelial cells. It was noticed that the poorly differentiated LD1 *Bscl2*$^{-/-}$ mammary gland alveolar epithelial cells had less polarity in WAP cellular distribution, which normally accumulates in the apical side of the differentiated alveolar epithelial cells. The poorly differentiated LD1 *Bscl2*$^{-/-}$ mammary gland alveoli had less percentage of larger lipid droplets, indicating impaired aggregation of lipid droplets into larger ones. These observations indicate that seipin plays an important role in mammary gland alveolar epithelial cell differentiation. The poorly differentiated LD1 *Bscl2*$^{-/-}$ mammary gland alveolar epithelial cells impair milk secretion, which contributes to reduced milk production in the *Bscl2*$^{-/-}$ lactating mice.

On the other hand, some LD1 *Bscl2*$^{-/-}$ mammary gland alveolar epithelial cells were well differentiated and had comparable cellular distribution of WAP with control. These cells had an accumulation of larger lipid droplets comparable to the control. A recent study in Drosophila and human cells [18] demonstrates that seipin forms discrete and dynamic foci in the ER that interact with nascent lipid droplets to enable their conversion into larger, mature lipid droplets. In the absence of seipin, most nascent lipid droplets often fail to grow, which is consistent with the smaller lipid droplets seen in the poorly differentiated LD1 *Bscl2*$^{-/-}$ mammary gland alveoli. Interestingly, it was also reported in the above study [18] that those lipid droplets that did grow, they eventually expanded into giant lipid droplets characteristic of seipin deficiency. The two patterns of lipid droplets observed in the poorly and well-differentiated LD1 *Bscl2*$^{-/-}$ mammary gland alveolar epithelial cells in this study may reflect both differentiation status and the function of seipin in lipid droplet growth.

LD1 *Bscl2*$^{-/-}$ mammary gland alveolar epithelial cells had normal proliferation but increased apoptosis, which led to the slough

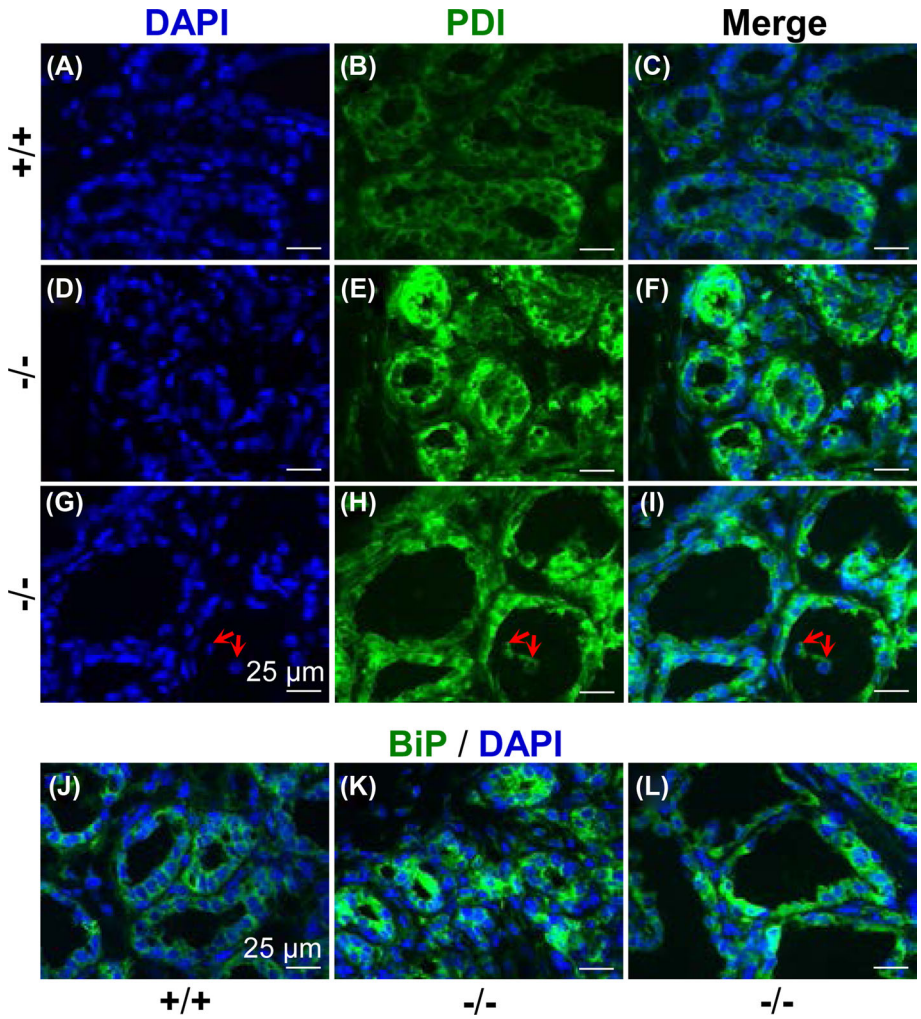

Figure 7. Increased expression of PDI and BiP in *Bscl2*$^{-/-}$ LD1 mammary gland alveolar epithelial cells. (A–C and J) Wild type (+/+), PDI (A–C), and BiP (J). (D–F and K) *Bscl2*$^{-/-}$ LD1 mammary gland with most retained alveolar epithelial cells, PDI (D–F), and BiP (K). (G–I and L) *Bscl2*$^{-/-}$ LD1 mammary gland with a few remaining alveolar epithelial cells, PDI (G–I), and BiP (L). Red arrows in G–I, sloughed epithelial cells in alveolar lumen; scale bar, 25 μm.

of many alveolar epithelial cells into the lumen and, subsequently, reduced alveolar epithelial cells for milk secretion. Accompanying with the increased apoptosis, there was increased ER stress in the LD1 *Bscl2*$^{-/-}$ mammary gland alveolar epithelial cells indicated by the increased expression of PDI and BiP, two ER chaperones induced during ER stress and important players in UPR pathway [26, 27]. Although it has been suggested that changes in ER stress pathway in the mammary gland during lactation are normal adaptions to the changing physiological state [28], and activation of UPR signaling pathway in responding to ER stress is initially protective [27], prolonged ER stress is proapoptotic [27]. One study reveals that mutant forms of seipin can activate the UPR pathway and induce ER stress-mediated cell death in cultured cells [26]. Another study indicates that protein phosphatase 1 (formerly 2C)-like (PP2Ce), an ER membrane targeted protein phosphatase, is highly expressed in lactating mammary gland epithelium and involved in regulating ER stress, and PP2Ce deficiency leads to loss of milk production and induction of lactating mammary gland epithelial apoptosis [29], indicating that ER stress plays an important role during lactation. The increased LD1 *Bscl2*$^{-/-}$ mammary gland alveolar epithelial cell apoptosis most likely results from increased ER stress.

ER stress was also induced in the mammary gland epithelium deficient of X-box binding protein 1 (Xbp1), a key mediator of UPR, and associated with inhibition of epithelial differentiation during lactation leading to impaired milk production [25]. It was possible that increased ER stress also contributed to the poor differentiation of some LD1 *Bscl2*$^{-/-}$ mammary gland alveolar epithelial cells.

In summary, this study reveals a novel in vivo role of seipin in lactation. Although seipin deficiency did not have obvious effects on cell proliferation of mammary gland alveolar epithelial cells or protein synthesis and lipid syntheses in the mammary gland alveolar epithelial cells, seipin deficiency led to poor differentiation and/or increased apoptosis of mammary gland alveolar epithelial cells, both of which contribute to reduced milk production and both of which could result from increased ER stress in the mammary gland alveolar epithelial cells. The molecular mechanisms of seipin in regulating ER stress during lactation remain to be elucidated.

Acknowledgments

The authors thank the Office of the Vice President for Research, Interdisciplinary Toxicology Program, and Department of Physiology and Pharmacology at the University of Georgia for support.

Conflict of Interest: The authors have declared that no conflict of interest exists.

References

1. Macias H, Hinck L. Mammary gland development. *Wiley Interdiscip Rev Dev Biol* 2012; **1**:533–557.
2. Schwertfeger KL, McManaman JL, Palmer CA, Neville MC, Anderson SM. Expression of constitutively activated Akt in the mammary gland leads to excess lipid synthesis during pregnancy and lactation. *J Lipid Res* 2003; **44**:1100–1112.
3. Chong BM, Reigan P, Mayle-Combs KD, Orlicky DJ, McManaman JL. Determinants of adipophilin function in milk lipid formation and secretion. *Trends Endocrinol Metab* 2011; **22**:211–217.
4. Stein O, Stein Y. Lipid synthesis, intracellular transport, and secretion. II. Electron microscopic radioautographic study of the mouse lactating mammary gland. *J Cell Biol* 1967; **34**:251–263.
5. Wu CC, Howell KE, Neville MC, Yates JR, 3rd, McManaman JL. Proteomics reveal a link between the endoplasmic reticulum and lipid secretory mechanisms in mammary epithelial cells. *Electrophoresis* 2000; **21**:3470–3482.
6. Le Parc A, Leonil J, Chanat E. AlphaS1-casein, which is essential for efficient ER-to-Golgi casein transport, is also present in a tightly membrane-associated form. *BMC Cell Biol* 2010; **11**:65.
7. Picariello G, Ferranti P, Mamone G, Klouckova I, Mechref Y, Novotny MV, Addeo F. Gel-free shotgun proteomic analysis of human milk. *J Chromatogr A* 2012; **1227**:219–233.
8. Magre J, Delepine M, Khallouf E, Gedde-Dahl T, Jr., Van Maldergem L, Sobel E, Papp J, Meier M, Megarbane A, Bachy A, Verloes A, d'Abronzo FH et al. Identification of the gene altered in Berardinelli-Seip congenital lipodystrophy on chromosome 11q13. *Nat Genet* 2001; **28**:365–370.
9. Bi J, Wang W, Liu Z, Huang X, Jiang Q, Liu G, Wang Y, Huang X. Seipin promotes adipose tissue fat storage through the ER Ca2+-ATPase SERCA. *Cell Metab* 2014; **19**:861–871.
10. Chen W, Chang B, Saha P, Hartig SM, Li L, Reddy VT, Yang Y, Yechoor V, Mancini MA, Chan L. Berardinelli-seip congenital lipodystrophy 2/seipin is a cell-autonomous regulator of lipolysis essential for adipocyte differentiation. *Mol Cell Biol* 2012; **32**:1099–1111.
11. Nolis T. Exploring the pathophysiology behind the more common genetic and acquired lipodystrophies. *J Hum Genet* 2014; **59**:16–23.
12. Szymanski KM, Binns D, Bartz R, Grishin NV, Li WP, Agarwal AK, Garg A, Anderson RG, Goodman JM. The lipodystrophy protein seipin is found at endoplasmic reticulum lipid droplet junctions and is important for droplet morphology. *Proc Natl Acad Sci USA* 2007; **104**:20890–20895.
13. Chen W, Yechoor VK, Chang BH, Li MV, March KL, Chan L. The human lipodystrophy gene product Berardinelli-Seip congenital lipodystrophy 2/seipin plays a key role in adipocyte differentiation. *Endocrinology* 2009; **150**:4552–4561.
14. Jiang M, Gao M, Wu C, He H, Guo X, Zhou Z, Yang H, Xiao X, Liu G, Sha J. Lack of testicular seipin causes teratozoospermia syndrome in men. *Proc Natl Acad Sci USA* 2014; **111**:7054–7059.
15. El Zowalaty AE, Baumann C, Li R, Chen W, De La Fuente R, Ye X. Seipin deficiency increases chromocenter fragmentation and disrupts acrosome formation leading to male infertility. *Cell Death Dis* 2015; **6**: e1817.
16. Li R, El Zowalaty AE, Chen W, Dudley EA, Ye X. Segregated responses of mammary gland development and vaginal opening to prepubertal genistein exposure in Bscl2(-/-) female mice with lipodystrophy. *Reprod Toxicol* 2015; **54**:76–83.
17. Cartwright BR, Goodman JM. Seipin: from human disease to molecular mechanism. *J Lipid Res* 2012; **53**:1042–1055.
18. Wang H, Becuwe M, Housden BE, Chitraju C, Porras AJ, Graham MM, Liu XN, Thiam AR, Savage DB, Agarwal AK, Garg A, Olarte MJ et al. Seipin is required for converting nascent to mature lipid droplets. *Elife* 2016; **5**:e16582.
19. Li R, Zhao F, Diao H, Xiao S, Ye X. Postweaning dietary genistein exposure advances puberty without significantly affecting early pregnancy in C57BL/6J female mice. *Reprod Toxicol* 2014; **44**:85–92.
20. Li R, Diao H, Zhao F, Xiao S, El Zowalaty AE, Dudley EA, Mattson MP, Ye X. Olfactomedin 1 deficiency leads to defective olfaction and impaired female fertility. *Endocrinology* 2015; **156**:3344–3357.
21. Xiao S, Diao H, Zhao F, Li R, He N, Ye X. Differential gene expression profiling of mouse uterine luminal epithelium during periimplantation. *Reprod Sci* 2014; **21**:351–362.
22. Diao H, Xiao S, Howerth EW, Zhao F, Li R, Ard MB, Ye X. Broad gap junction blocker carbenoxolone disrupts uterine preparation for embryo implantation in mice. *Biol Reprod* 2013; **89**:31.
23. Zowalaty AEE, Ye X. Seipin deficiency leads to defective parturition in mice. *Biol Reprod* 2017; **97**:378–386.
24. Langlois D, Forcheron F, Li JY, del Carmine P, Neggazi S, Beylot M. Increased atherosclerosis in mice deficient in perilipin1. *Lipids Health Dis* 2011; **10**:169.
25. Hasegawa D, Calvo V, Avivar-Valderas A, Lade A, Chou HI, Lee YA, Farias EF, Aguirre-Ghiso JA, Friedman SL. Epithelial Xbp1 is required for cellular proliferation and differentiation during mammary gland development. *Mol Cell Biol* 2015; **35**:1543–1556.
26. Ito D, Suzuki N. Seipinopathy: a novel endoplasmic reticulum stress-associated disease. *Brain* 2009; **132**:8–15.
27. Perri ER, Thomas CJ, Parakh S, Spencer DM, Atkin JD. The unfolded protein response and the role of protein disulfide isomerase in neurodegeneration. *Front Cell Dev Biol* 2015; **3**:80.
28. Invernizzi G, Naeem A, Loor JJ. Short communication: endoplasmic reticulum stress gene network expression in bovine mammary tissue during the lactation cycle1. *J Dairy Sci* 2012; **95**:2562–2566.
29. Ren S, Lu G, Ota A, Zhou ZH, Vondriska TM, Lane TF, Wang Y. IRE1 phosphatase PP2Ce regulates adaptive ER stress response in the postpartum mammary gland. *PLoS One* 2014; **9**:e111606.